

## Highlights

### **Colab NAS: Obtaining lightweight task-specific convolutional neural networks following Occam's razor**

Andrea Mattia Garavagno, Daniele Leonardis, Antonio Frisoli

- Hardware Aware NAS for task-specific convolutional neural networks
- A novel low-cost derivative-free search strategy inspired by Occam's razor
- State-of-the-art results on the Visual Wake Word dataset in just 4.5 GPU hours
- Able to be executed on free subscription online GPU services

# Colab NAS: Obtaining lightweight task-specific convolutional neural networks following Occam's razor

Andrea Mattia Garavagno<sup>a</sup>, Daniele Leonardis<sup>a</sup>, Antonio Frisoli<sup>a</sup>

<sup>a</sup>*Institute of Mechanical Intelligence, Scuola Superiore Sant'Anna of Pisa, Piazza Martiri della Libertà, 33, Pisa, 56127, Tuscany, Italy*

---

## Abstract

The current trend of applying transfer learning from CNNs trained on large datasets can be an overkill when the target application is a custom and delimited problem with enough data to train a network from scratch. On the other hand, the training of custom and lighter CNNs requires expertise, in the from-scratch case, and/or high-end resources, as in the case of hardware-aware neural architecture search (HW NAS), limiting access to the technology by non-habitual NN developers.

For this reason, we present Colab NAS, an affordable HW NAS technique for producing lightweight task-specific CNNs. Its novel derivative-free search strategy, inspired by Occam's razor, allows it to obtain state-of-the-art results on the Visual Wake Word dataset in just 4.5 GPU hours using free online GPU services such as Google Colaboratory and Kaggle Kernel.

**Keywords:** TinyML, hardware-aware neural architecture search, visual wake words, lightweight convolutional neural networks

---

## 1. Introduction

Task-specific convolutional neural networks (CNN) are enabling the rise of next-generation smart wearable systems and distributed sensors. The limited size of the problem to be solved allows for lightweight models which fit the resource constraints of commodity electronics used in such devices. However, developing from scratch a good lightweight neural network model is not easy. A recent research area named hardware-aware Neural Architecture Search (HW NAS) is facing the problem, of tailoring the search to the precise resources of the target hardware. As of today, open-source projects such as MCUNet [1] and Micronets [2] are able to produce state-of-the-art TinyML models in around 300 GPU hours. Nevertheless, the majority of lightweight task-specific CNN are currently designed using Transfer Learning (TL). This is evident from research. Most papers which report the keywords “convolutional neural network” and “lightweight” in the title use pre-trained neural networks to design their application.

For example Sanida et al. [3], in 2022, proposed a lightweight task-specific CNN able to diagnose COVID-19 by evaluating chest X-rays. To design the network the transfer learning procedure is applied. MobileNetV2 by Sandler et al. [4] is used as the model backbone.

A similar approach is applied by Liu et al. [5], in 2022, to detect ships in spaceborne synthetic aperture radar (SAR) images. In this case, MobileNetV2 is used as a backbone for a YOLOv4-LITE model.

In the same year, transfer learning is also applied by Wang et al. [6] to develop a model based on Efficientnet-B1 [7], able to detect arc fault in photovoltaic systems, by analyzing power

spectrum images; by Khaki et al. [8] to develop a model based on MobileNetV2 able to detect and count wheat heads by analyzing pictures; and by Jubair et al. [9] to develop a model based on EfficientNet-B0 [7] able to early detect oral cancer by pictures of the oral cavity.

Ragusa et al. used MobileNets as a backbone for performing image polarity detection using visual attention [10] and for performing affordance detection [11] on embedded devices.

The above represents a brief overview of the rich literature involving lightweight task-specific neural network designs, using transfer learning, presented just in 2022.

Transfer learning uses the knowledge acquired by a CNN in solving a problem, to solve another similar one, reducing the training data and the time required to solve it. This technique helps when there is not enough data and/or time to design a model from scratch. On the contrary, TL can be an overkill: task-specific problems can be coped with by significantly lighter CNNs. Even the lightest models, used in the transfer learning procedure, are trained on large-scale datasets (i.e. ImageNet1k by Deng et al. [12]). In addition, in the case of application to specific problems, related datasets are often already available for the end-users. Generating a CNN from scratch seems then a convenient choice. Yet the search cost of HW NAS, or the cost of manual design, is still too high compared to the time required by TL, possibly explaining the prominent use of TL over HW NAS in the literature.

In this paper, we propose Colab NAS, an affordable hardware-aware NAS technique for producing lightweight task-specific CNNs. It uses a novel derivative-free search strategy, inspired by Occam's razor, that allows it to obtain state-of-the-art results on the Visual Wake Word dataset [13] in just 4.5 GPU hours using free online GPU services such as Google Colaboratory and Kaggle Kernel. Such a feature inspired its name, which wants

---

*Email address:* AndreaMattia.Garavagno@santannapisa.it  
(corresponding author) (Andrea Mattia Garavagno)

to emphasise the ability to be run on free subscription online services, making its use available to everyone. We believe this feature is critical to foster the use of CNNs in the variety of application tasks they can adapt, especially in the field of embedded wearable and distributed devices, and implemented by a heterogeneous population of end-users and researchers.

In this paper, we present details of the proposed technique and experimental validation on four different classification problems on online-available datasets. Then, the results obtained on the Visual Wake Word dataset are compared with state-of-the-art HW NAS methods. We provide online access to experimental data and code in the form of Google Colaboratory notebooks at this [link](#).

## 2. Related Works

In recent years standard benchmarks for tiny machine learning applications were established [14]. Imagenet1k, by Deng et al. [12], and the Visual Wake Words, by Chowdhery et al. [13], datasets were chosen to measure the performance of the most recent efforts of trying to implement deep-learning techniques for computer vision tasks on commodity hardware.

These efforts followed the path opened by manually designed lightweight models such as MobileNets [28] [29] [30], SqueezeNet [31], ShuffleNets [32] [33], and tried to automatize the design using Neural Architecture Search techniques, taking into consideration hardware constraints such as Flash and SRAM occupancy, or latency, giving birth to what is called hardware aware Neural Architecture Search. Among the most recent notable projects, there are MCUNet, Micronets and MNASNet.

MNASNet [25] tries to find the Pareto optimal solution of an objective function penalized by hardware constraints using reinforcement learning. The search space is hierarchical; at each iteration, an RNN, the controller, produces a sample architecture which is trained, for evaluating the accuracy, and then executed on the target hardware to evaluate the latency.

MCUNet [1] [24] is composed of two parts an HW-NAS technique called TinyNAS, and a framework for executing deep learning on microcontrollers called TinyEngine. TinyNAS makes use of an evolutionary algorithm to explore a search space composed of a supernet, which contains a multitude of possible networks to use. The search space is built considering the hardware constraints. Flash, SRAM occupancy and latency are taken into account and measured directly on the target hardware.

The idea of sharing the weights of different architectural solutions in a single supernet, by combining different paths, has been pioneered by DARTS [26] and ProxylessNAS [27] to reduce the search cost by reducing the number of trainings required.

Also, Micronets [2] employs the concept of supernet. This time a gradient-based method, called Differentiable Neural Architecture Search (DNAS), introduced by Liu et al. [26], is used to explore the search space, looking for models with low memory usage and low op count, where op count is treated as a viable proxy to latency, avoiding hardware in the loop.

Our solution does not use controllers or genetics algorithms to explore the search space, and neither uses DNAS. It introduces a novel derivative-free method, inspired by Occam’s razor, to explore the search space. Such a search strategy allows us to significantly reduce the search cost of our NAS.

## 3. Colab NAS

This section describes the developed technique to search lightweight, task-specific CNNs.

Every HW NAS technique has three unique identification factors: the search space, the optimization problem formulation and the search strategy.

The search space defines the means of the search, i.e. the rules and set of the network’s architectural elements that will be used to build the solution. The optimization problem establishes the boundaries of the research and the logic used to evaluate each solution. Finally, the search strategy describes the way the search space is explored, i.e. how the problem solution is found.

### 3.1. Search Space and Problem Formulation

There are three types of search spaces: layer-wise, cell-wise and hierarchical. Colab NAS uses a cell-wise search space. It starts from a single bidimensional convolutional layer. Then, it continues by stacking couples of pooling and convolutional layers, which form a single cell as shown in figure 1, until the network’s generalization capability doesn’t stop increasing.

The stopping criterion takes inspiration from the problem-solving principle that “entities should not be multiplied beyond necessity”, also known as Occam’s razor, attributed to English Franciscan friar William of Ockham, who lived between the thirteen and the fourteenth century.

The number of kernels of each cell added is determined by the following equation, where  $k$  represents the number of kernels used in the first convolutional layer.

$$k^i = \begin{cases} k & \text{if } i = 0 \\ 2 \cdot k^0 & \text{if } i = 1 \\ \left[ k^{i-1} \cdot (2 - \sum_{n=1}^{i-1} 2^{-n}) \right] & \text{if } i > 1 \end{cases} \quad (1)$$

The search space is constrained by the number of parameters of the network and the number of Floating Point Operations (FLOPs). The former is used as a rough estimate of the ROM memory occupation of the network, the latter as a rough estimate of latency as suggested by Banbury et al. [2]. RAM occupancy is not taken into account in this model since it strongly depends on the framework used to deploy the network on the target hardware.

$$P : \begin{cases} \max f(k, c, \bar{v}i) \\ \phi_P(k, c, \bar{v}i) \leq \xi_P \\ \phi_F(k, c, \bar{v}i) \leq \xi_F \\ \xi_P, \xi_F > 0 \end{cases} \quad (2)$$

This leads to the problem formulation 2, where function  $f$  returns the mean validation accuracy during the last ten epochs

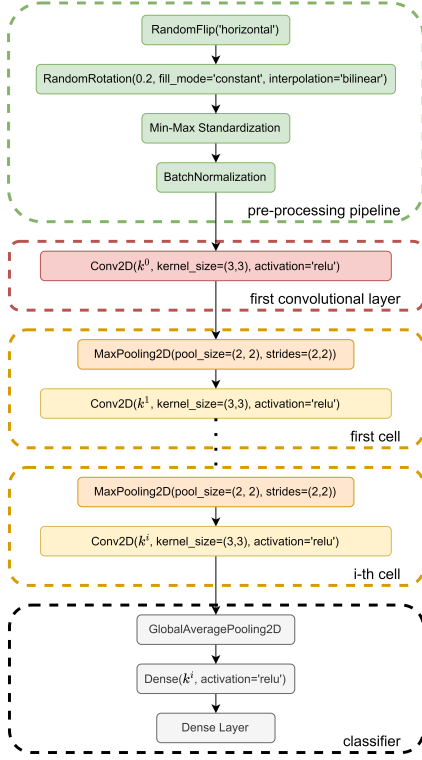


Figure 1: Detailed graphical representation of the network architecture.  $k_i$  represents the number of kernels used in the  $i$ -th cell. Instead, the dotted connection represents a generic number of cells added. The deep dense layer has a number of neurons equal to the kernels used in the last addition.

of training; function  $\phi_P$  the number of network's parameters; function  $\phi_F$  the number of FLOPs. These depend on the number of kernels used in the first layer  $k$ , the number of cells added  $c$ , and the magnitude of the network's input volume  $v_i$ .  $f(k, c, \bar{v}_i)$  values come from training.

The network's input volume is considered fixed during the research since it depends on the user's needs. Hence the search variable  $x = (k, c)$  is defined, reformulating the problem as indicated in 3. The feasible search space is indicated as  $\Omega$ .

$$P1 : \begin{cases} \max f(x) \\ \phi_P(x) \leq \xi_P \\ \phi_F(x) \leq \xi_F \\ \xi_P, \xi_F > 0 \end{cases} \quad (3)$$

### 3.2. Network's Architecture details

Some architectural choices are fixed. All the convolutional layers have 3x3 kernels and use zero padding to preserve the input volume. Instead, the pooling layers have 2x2 receptive field size and use (2, 2) stride.

The convolutional base output is reduced by applying the 2D Global Average Pooling operator to improve the model's generalization capability [17]. Subsequently, a deep fully connected layer, having the number of neurons equal to the number of kernels of the last convolutional layer, further elaborates the reduced features. Finally, a single fully connected layer classifies the extracted features.

A pre-processing pipeline is included in the network's architecture. It first applies min-max standardization, to improve gradient descent convergence rate [18]. Then, uses batch normalization to stabilize and speed up the training [19]. Data augmentation is also applied. Both horizontal flips and random rotations are used. Figure 1 graphically represents the generic architecture used as a search space.

### 3.3. Search Strategy

The search strategy explores the search space in two steps. First, as stated before, given a starting number of kernels of the first layer, it starts to add cells until the network's generalization capability does not stop increasing, according to Occam's razor, or until the network respects hardware constraints. Then it repeats the latter process changing the number of kernels of the first layer according to equation 4.

$$k_j = \begin{cases} k & \text{if } j = 0 \\ 2 \cdot k_0 & \text{if } j = 1 \\ 2 \cdot k_{j-1} & \text{if } f(k_1^*, c_1^*) > f(k_0^*, c_0^*) \\ \frac{1}{2} \cdot k_{j-1} & \text{if } f(k_1^*, c_1^*) \leq f(k_0^*, c_0^*) \end{cases} \quad (4)$$

If the hardware selected for deployment allows, the process is repeated with double the number of kernels. If the solution found at the second iteration ( $k_1^*, c_1^*$ ) is better than the previous one ( $k_0^*, c_0^*$ ), the process continues in the same way until performance does not improve anymore, or the hardware limits are reached. Otherwise, the process continues by halving down the initial number of kernels until performance degradation is met. Also this time Occam's razor is respected. Entities are not multiplied beyond necessity.

Such a search strategy can be interpreted as a custom derivative-free method for solving the constrained optimization problem presented in equation 3. Algorithm 1 describes such an interpretation.

It is an alternating search in the direction of the two main axes, as shown in figure 2. First, it explores the axis of the cells' additions (direction  $d = (0, 1)$ ) given a starting point, using algorithm 2. Then it moves the starting point on the axis of the number of kernels of the first layer (direction  $d = (1, 0)$ ) and repeats the search.

If the hardware selected for deployment allows, the number of kernels used in the first layer is doubled, i.e. the starting point  $x_0$  is doubled. If the network found with the new starting point is better than the previous one, the algorithm continues doubling the starting point until the generalization capability does not improve anymore, or the hardware limits are reached. Otherwise, the algorithm continues by halving down the initial number of kernels, i.e. the starting point  $x_0$ , until performance degradation is met or an unfeasible point is found.  $\tilde{x}_j$  represents the algorithm's output.

Procedure 2 explores the axis of the cells' additions ( $d = (0, 1)$ ) given a starting point  $x$ , with a unitary step size ( $t = 1$ ). Practically, it continues to add cells until the generalization capability does not stop increasing, or until the new network is feasible.

**Algorithm 1** Search Strategy**Require:**  $x_0 \in \Omega$ 

**Ensure:**  $\begin{cases} f(\tilde{x}_j) > f(\tilde{x}_{j-1}), \tilde{x}_j \in \Omega & \text{always} \\ f(\tilde{x}_{j+1}) \leq f(\tilde{x}_j) & \text{if } \tilde{x}_{j+1} \in \Omega \end{cases}$

$\epsilon \leftarrow 0.005, k_0 \leftarrow 4, x_0 \leftarrow (k_0, 0), d \leftarrow (1, 0), t_0 \leftarrow x_0, j \leftarrow 0$   
 $\tilde{x}_0 = \text{EXPLORE\_NUM\_CELLS}(x_0)$   
 $x_1 = x_0 + t_0 \cdot d$   
 $\tilde{x}_1 = \text{EXPLORE\_NUM\_CELLS}(x_1)$   
**if**  $f(\tilde{x}_1) > f(\tilde{x}_0)$  **and**  $x_1 \in \Omega$  **then**  
  **do**  
     $j = j + 1$   
     $t_j = x_j$   
     $x_{j+1} = x_j + t_j \cdot d$   
     $\tilde{x}_{j+1} = \text{EXPLORE\_NUM\_CELLS}(x_{j+1})$   
    **while**  $f(\tilde{x}_{j+1}) > f(\tilde{x}_j) + \epsilon$  **and**  $x_{j+1} \in \Omega$   
  **else**  
     $x_1 = x_0$   
    **do**  
       $j = j + 1$   
       $t_j = -\frac{x_j}{2}$   
       $x_{j+1} = x_j + t_j \cdot d$   
       $\tilde{x}_{j+1} = \text{EXPLORE\_NUM\_CELLS}(x_{j+1})$   
      **while**  $f(\tilde{x}_{j+1}) \geq f(\tilde{x}_j)$  **and**  $x_{j+1} \in \Omega$   
    **end if**  
**Output:**  $\tilde{x}_j$

**Algorithm 2** EXPLORE\_NUM\_CELLS( $x$ )**Require:**  $x \in \Omega$ 

**Ensure:**  $\begin{cases} f(x_i) > f(x_{i-1}), x_i \in \Omega & \text{always} \\ f(x_{i+1}) \leq f(x_i) & \text{if } x_{i+1} \in \Omega \end{cases}$

$x_0 \leftarrow x, d \leftarrow (0, 1), t \leftarrow 1, i \leftarrow 0$   
**do**  
   $x_{i+1} = x_i + t \cdot d$   
   $i = i + 1$   
**while**  $f(x_{i+1}) > f(x_i)$  **and**  $x_{i+1} \in \Omega$   
**return**  $x_i$

For the sake of synthesis, in algorithm 1,  $x_1$  is explored in any case, even if it is not feasible. For the same reason the feasibility check for the point  $x_{j+1}$  is done after the exploration. Something similar happens in algorithm 2, where the network  $x_{i+1}$  is trained even if it is not feasible.

**4. Experimental Methods**

Four task-specific classification problems are chosen to demonstrate the efficacy of the proposed technique. The resulting models are compared with the ones obtained by applying transfer learning.

Also, a comparison with state-of-the-art hardware-aware NAS, based on the Visual Wake Word dataset, a standard TinyML benchmark [14], is presented.

Code and datasets are publicly available in the form of Google Colaboratory's notebooks at the link in section 1. All the computations have been executed on Google Colaboratory using Tesla T4 GPUs, as of today, the ones mostly offered to free subscription users.

In all four classification problems, 10% of data is reserved for validation and not used for training. All the images are resized to 224x224 resolution.

The design and training of convolutional neural networks are performed using the Keras backend of Tensorflow.

Regarding the training details, a learning rate of  $10^{-3}$  and  $10^2$  epochs are used. The optimizer used is Adam by Kingma et al. [20].

A small batch size of 8 samples is used to increase the network's generalization capability, avoiding sharp minima [23].

**4.1. Melanoma Skin Cancer**

The melanoma skin cancer classification task aims to discriminate between benign and malignant images of melanoma skin cancer. It contains 5.500 benign and 5.105 malignant images of melanoma skin cancer. It is publicly available on kaggle under the name of Melanoma Skin Cancer Dataset of 10000 Images <sup>1</sup>.

<sup>1</sup><https://www.kaggle.com/datasets/hasnainjaved/melanoma-skin-cancer-dataset-of-10000-images?resource=download>

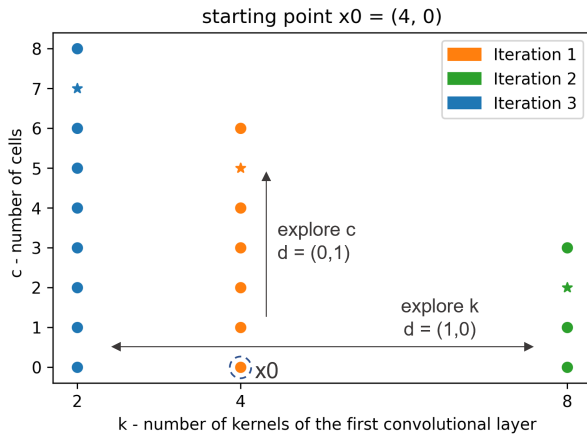


Figure 2: A figure that is showing the points explored by the algorithm during a sample run, in which the generalization capability does not increase during iteration 1 and gets worse during iteration 2. The star marker represents the network with the highest generalization capability for each iteration. As you can see, during each iteration the points move along the c axis. After each iteration, the starting point moves along the k axis.

#### 4.2. Human Recognition

The human recognition classification task aims to discriminate between images with and without human presence. It is composed of 10,000 images equally distributed between the two cases. The images used are taken from the training split of Visual Wake Word dataset by Chowdhery et al. [13].

#### 4.3. Flowers-4

The Flowers-4 classification task aims to discriminate between four classes of flowers: dandelion, iris, tulip, and magnolia. It contains 1052 instances of dandelion, 1054 instances of iris, 1048 instances of tulip, and 1048 instance of magnolia. It is a subset of the Flowers dataset, which is publicly available on kaggle<sup>2</sup>.

#### 4.4. Animals-3

The Animals-3 classification task aims to discriminate between three species of animals: horse, butterfly and hen. It contains 2623 instances of horses, 2112 instances of butterflies, and 3098 instances of hens. It is a subset of the Animals-10 dataset, which is publicly available on kaggle<sup>3</sup>.

### 5. Results

This section presents the results obtained by applying the technique to the four selected classification tasks. 2,259,277 parameters and 599,212,056 FLOPs are set as hardware constraints, which are the equivalent of using MobileNetV2 as a feature extractor with one dense layer with four neurons as a classifier.

The results are in form of a table. Each table reports architectural details such as the number of kernels used in each cell added,  $N_{kernels}$ , the number of parameters of each solution, "Params", and the number of floating point operations, "FLOPs". Finally, the mean test accuracy obtained during the last ten epochs of training is reported under the name "Score". The architectural solution found is highlighted in grey.

Each run of the algorithm is under the 12 hours execution limit, for free subscription users, of Google Colaboratory<sup>4</sup>.

In the next section, the networks highlighted in grey will be compared to the ones obtained by applying the transfer learning technique on the same task.

#### 5.1. Melanoma Skin Cancer

Regarding the Melanoma Skin Cancer classification task the algorithm took 3 iterations to finish, taking 9.3 hours of execution on Google Colaboratory. The best score has been obtained during the first iteration, as highlighted in light grey in the following table.

<sup>2</sup><https://www.kaggle.com/datasets/l31lff/flowers>

<sup>3</sup><https://www.kaggle.com/datasets/alessiocorrado99/animals10>

<sup>4</sup>Resources are not guaranteed and not unlimited, and the usage limits sometimes fluctuate. This is necessary for Colaboratory to be able to provide resources free of charge.

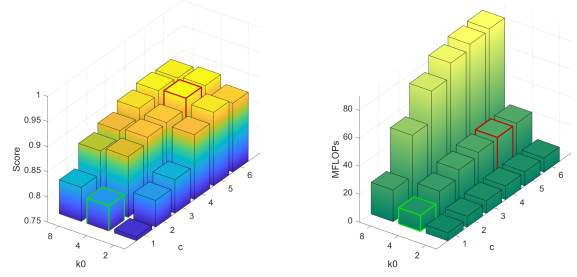


Figure 3: Results of the architecture search on the Melanome Skin Cancer dataset. Green edges indicate the starting point, red edges the end point of the search

Iteration 1 ( $k_0 = 4$ )					
c	$N_{kernels}$	Params	FLOPs	Score	GPU Time
0	4	149	11,389,997	0.801	0:29:49
1	8	501	18,816,153	0.871	0:29:35
2	12	1,465	24,310,597	0.882	0:29:27
3	15	3,187	26,874,448	0.884	0:28:58
4	17	5,567	27,780,886	0.905	0:29:50
5	19	8,569	28,067,784	0.903	0:30:14

Iteration 2 ( $k_0 = 8$ )					
c	$N_{kernels}$	Params	FLOPs	Score	GPU Time
0	8	317	22,629,529	0.818	0:29:30
1	16	1,693	51,932,721	0.863	0:31:13
2	24	5,509	73,759,945	0.876	0:31:46
3	30	12,355	83,968,291	0.893	0:32:47
4	34	21,833	87,580,703	0.901	0:32:41
5	37	33,411	88,694,320	0.899	0:33:12

Iteration 3 ( $k_0 = 2$ )					
c	$N_{kernels}$	Params	FLOPs	Score	GPU Time
0	2	77	5,770,255	0.758	0:28:26
1	4	169	7,676,973	0.803	0:28:56
2	6	415	9,069,403	0.817	0:28:24
3	8	887	9,759,385	0.879	0:28:34
4	9	1,563	10,016,966	0.896	0:30:04
5	10	2,404	10,097,367	0.887	0:31:03

#### 5.2. Human Recognition

Instead, the Human Recognition classification task obtained the best score during the second iteration. It took 9.8 hours of execution on Google Colaboratory to finish.

Iteration 1 ( $k_0 = 4$ )					
c	$N_{kernels}$	Params	FLOPs	Score	GPU Time
0	4	149	11,389,997	0.567	0:28:43
1	8	501	18,816,153	0.656	0:28:11
2	12	1,465	24,310,597	0.738	0:28:10
3	15	3,187	26,874,448	0.755	0:28:34
4	17	5,567	27,780,886	0.746	0:29:10



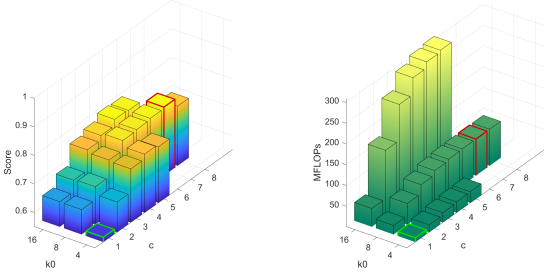


Figure 4: Results of the architecture search on the Human Recognition dataset. Green edges indicate the starting point, red edges the end point of the search

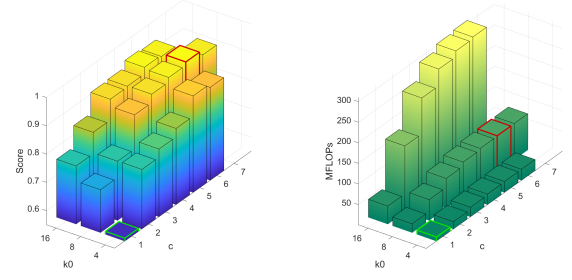


Figure 5: Results of the architecture search on the Animals dataset. Green edges indicate the starting point, red edges the end point of the search

Iteration 2 ( $k_0 = 8$ )					
c	$N_{kernels}$	Params	FLOPs	Score	GPU Time
0	8	317	22,629,529	0.637	0:28:55
1	16	1,693	51,932,721	0.683	0:30:07
2	24	5,509	73,759,945	0.742	0:30:43
3	30	12,355	83,968,291	0.776	0:30:16
4	34	21,833	87,580,703	0.78	0:31:23
5	37	33,411	88,694,320	0.785	0:30:46
6	39	46,593	88,928,617	0.79	0:33:26
7	40	60,754	88,956,743	0.759	0:35:03

Iteration 3 ( $k_0 = 16$ )					
c	$N_{kernels}$	Params	FLOPs	Score	GPU Time
0	16	749	45,108,785	0.638	0:28:14
1	32	6,189	161,518,689	0.679	0:31:23
2	48	21,373	248,526,481	0.751	0:31:13
3	60	48,673	289,265,749	0.767	0:32:04
4	68	86,501	303,688,717	0.789	0:32:10
5	73	131,965	308,075,544	0.786	0:32:41

### 5.3. Animals-3

Also, the Animals-3 classification task obtained the best score during the second iteration, taking 8.7 hours on Google Colaboratory to finish.

Iteration 1 ( $k_0 = 4$ )					
c	$N_{kernels}$	Params	FLOPs	Score	GPU Time
0	4	159	11,390,030	0.561	0:24:39
1	8	519	18,816,202	0.761	0:24:53
2	12	1,491	24,310,662	0.79	0:26:10
3	15	3,219	26,874,525	0.82	0:26:56
4	17	5,603	27,780,971	0.892	0:26:44
5	19	8,609	28,067,877	0.879	0:27:05

Iteration 2 ( $k_0 = 8$ )					
c	$N_{kernels}$	Params	FLOPs	Score	GPU Time
0	8	335	22,629,578	0.702	0:26:24
1	16	1,727	51,932,802	0.76	0:26:32
2	24	5,559	73,760,058	0.881	0:27:57
3	30	12,417	83,968,428	0.911	0:25:53
4	34	21,903	87,580,856	0.927	0:27:31
5	37	33,487	88,694,485	0.939	0:28:06
6	39	46,673	88,928,790	0.921	0:29:32

Iteration 3 ( $k_0 = 16$ )					
c	$N_{kernels}$	Params	FLOPs	Score	GPU Time
0	16	783	45,108,866	0.756	0:25:38
1	32	6,255	161,518,834	0.832	0:27:31
2	48	21,471	248,526,690	0.906	0:28:19
3	60	48,795	289,266,006	0.909	0:28:09
4	68	86,639	303,689,006	0.933	0:27:48
5	73	132,113	308,075,853	0.928	0:27:44

### 5.4. Flowers-4

Finally, the Flower-4 classification task obtained the best score during the third iteration, but the variation was not sufficient to overcome  $\epsilon = 0.005$ , hence the resulting network is the one obtained during the second iteration. The algorithm took 4.4 hours on Google Colaboratory to finish.

Iteration 1 ( $k_0 = 4$ )					
c	$N_{kernels}$	Params	FLOPs	Score	GPU Time
0	4	164	11,390,044	0.801	0:14:04
1	8	528	18,816,224	0.837	0:12:48
2	12	1,504	24,310,692	0.867	0:13:27
3	15	3,235	26,874,561	0.897	0:13:35
4	17	5,621	27,781,011	0.915	0:13:51
5	19	8,629	28,067,921	0.91	0:13:53

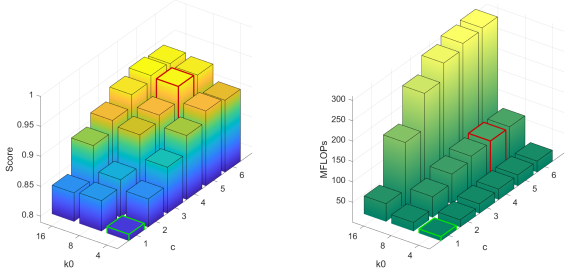


Figure 6: Results of the architecture search on the Flowers dataset. Green edges indicate the starting point, red edges the end point of the search

Iteration 2 ( $k_0 = 8$ )					
c	$N_{kernels}$	Params	FLOPs	Score	GPU Time
0	8	344	22,629,600	0.841	0:14:13
1	16	1,744	51,932,840	0.853	0:13:41
2	24	5,584	73,760,112	0.905	0:14:09
3	30	12,448	83,968,494	0.915	0:14:36
4	34	21,938	87,580,930	0.94	0:17:06
5	37	33,525	88,694,565	0.936	0:14:36

Iteration 3 ( $k_0 = 16$ )					
c	$N_{kernels}$	Params	FLOPs	Score	GPU Time
0	16	800	45,108,904	0.838	0:13:17
1	32	6,288	161,518,904	0.894	0:13:44
2	48	21,520	248,526,792	0.913	0:14:23
3	60	48,856	289,266,132	0.933	0:14:23
4	68	86,708	303,689,148	0.942	0:14:58
5	73	132,187	308,076,005	0.939	0:14:39

## 6. Comparison with the networks obtained using Transfer Learning

This section compares the networks obtained in section 5, the ones highlighted in grey, to the ones obtained by applying transfer learning.

The metrics used for the comparison are the mean test accuracy obtained during the last ten epochs of training, called “Score”, the number of parameters “Params”, and the number of FLOPs computed by the Keras API.

MobileNetV2, with frozen weights trained on ImageNet1k, is used as the backbone for the transfer learning technique. The extracted features are compressed by a bi-dimensional global average pooling layer and then given to a shallow classifier, composed of only one dense layer.

The pre-processing pipeline is the same as the one used with the NAS, reported in section 3. It first applies both horizontal flips and random rotations, then applies min-max standardization, and finally uses batch normalization.

Such models are trained for 10 epochs using a learning rate of  $10^{-3}$ .

### 6.1. Melanoma Skin Cancer

For the Melanoma Skin Cancer classification task, the NAS outperformed the result obtained by applying transfer learning

by all means. The obtained network is 405.8 times lighter and 0.089 more precise than the one obtained by applying transfer learning. Moreover, it performs 21.6 times fewer FLOPs.

	TL	NAS
Params	2,259,277	5,567
FLOPs	599,204,353	27,780,886
Score	0.816	0.905

### 6.2. Human Recognition

In the case of the Human Recognition classification task, the NAS produced a model that is 48.5 times lighter but 0.079 less precise than the one obtained by applying transfer learning. However, it performs 6.7 times fewer FLOPs.

	Transfer Learning	NAS
Params	2,259,277	46,593
FLOPs	599,204,353	88,928,617
Score	0.869	0.792

### 6.3. Animals-3

For the Animals-3 classification task, the NAS produced a model that is 67.5 times lighter but 0.05 less precise than the one obtained by applying transfer learning. However, it performs 6.8 times fewer FLOPs.

	Transfer Learning	NAS
Params	2,261,839	33,487
FLOPs	599,209,490	88,694,485
Score	0.989	0.939

### 6.4. Flowers-4

Finally, for the Flowers-4 classification task, the NAS produced a model that is 103.1 times lighter but 0.032 less precise than the one obtained by applying transfer learning. However, it performs 6.8 times fewer FLOPs.

	Transfer Learning	NAS
Params	2,263,120	21,938
FLOPs	599,212,056	87,580,930
Score	0.972	0.94

## 7. Comparison with state-of-the-art hardware-aware NAS techniques on the Visual Wake Word dataset

This section presents the comparison of the proposed NAS with state-of-the-art hardware-aware NAS techniques for convolutional neural networks. It proposes a comparison between two different projects: MicroNets by Banbury et al. [2] and MCUNet by Lin et al. [1] [24].

The comparison is based on the Visual Wake Word dataset [13], a standard benchmark for TinyML models [14]. Imagenet1k [12] is not included, given its general-purpose nature,



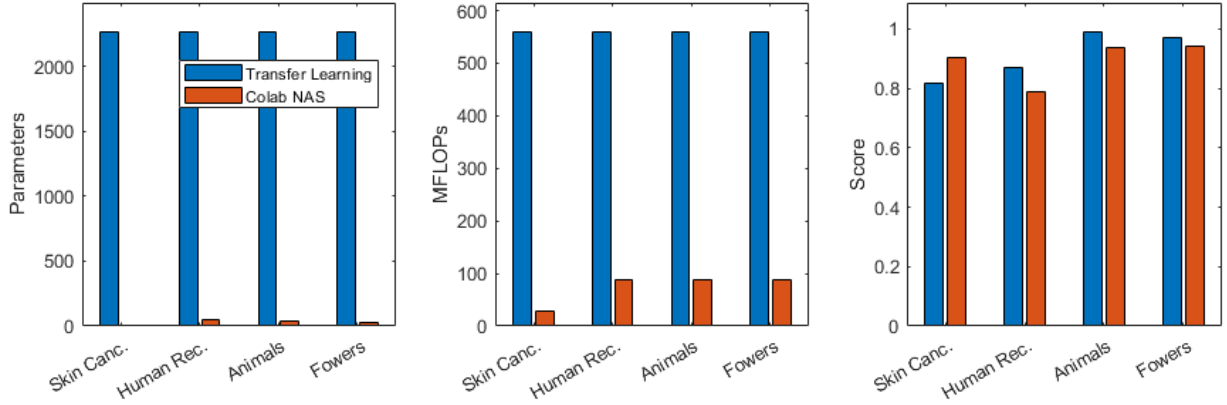


Figure 7: Performance comparison between Transfer Learning method (using MobileNetV2) and our proposed NAS.

which is not compatible with the task-specific nature of our method.

Only the lightest model has been selected from both projects. In the case of MicroNets the “vwv2\_50\_50\_INT8.tflite” model has been downloaded from the ARM’s GitHub web page <sup>5</sup>. The test accuracy was taken from their GitHub <sup>6</sup>.

In the case of MCUNet, the “mcunet-10fps-vwv” model has been downloaded from the laboratory’s web page <sup>7</sup>. The test accuracy was taken from their GitHub <sup>8</sup>.

Instead, our model is obtained by applying the NAS technique to one-tenth of the visual wake word training set, and then by training the resulting architecture onto the whole training set. In both cases, one-tenth of the data is used for validation.

The constraints are the same used in section 5. Also, the pre-processing pipeline is the same. The only thing that changes is the input volume which is taken to 50x50x3.

The following table reports the NAS’ iterations as done in section 5. The resulting network is highlighted in grey. The algorithm took 4.5 hours to finish.

Iteration 1					
c	$N_{kernels}$	Params	FLOPs	Score	GPU Time
0	4	149	567,545	0.614	0:19:53
1	8	501	937,653	0.678	0:18:24
2	12	1,465	1,189,721	0.693	0:19:39
3	15	3,187	1,307,612	0.689	0:23:13

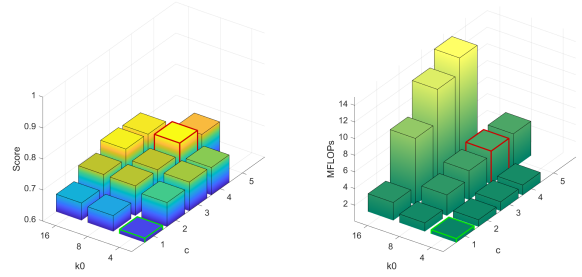


Figure 8: Results of the architecture search on the Visual Wake Words dataset. Green edges indicate the starting point, red edges the end point of the search

Iteration 2					
c	$N_{kernels}$	Params	FLOPs	Score	GPU Time
0	8	317	1,127,653	0.651	0:18:34
1	16	1,693	2,588,061	0.696	0:18:52
2	24	5,509	3,590,181	0.697	0:17:51
3	30	12,355	4,059,567	0.732	0:19:33
4	34	13,487	4,225,943	0.709	0:24:06

Iteration 3					
c	$N_{kernels}$	Params	FLOPs	Score	GPU Time
0	16	749	2,248,061	0.656	0:19:22
1	32	6,189	8,049,645	0.697	0:18:52
2	48	21,373	12,045,821	0.728	0:19:53
3	60	48,673	13,919,009	0.725	0:26:36

All the models are in TFLite format. They are fully quantized to perform 8-bit inference. Since there is no direct way to measure FLOPs using the TFLite API, no value for them is presented. To have a comparison of the execution times, a latency value is measured using the IPython magic command “%timeit” alongside the TFLite interpreter invocation. The input tensor content is random.

All the measurements were performed during the same Google Colaboratory session with a dual-core Intel(R) Xeon(R) CPU at 2.20GHz. No GPU was involved.

The next table shows the comparison. The Flash occupancy corresponds to the file weight, while the input volume was read

<sup>5</sup>[https://github.com/ARM-software/ML-zoo/blob/master/models/visual\\_wake\\_words/micronet\\_vwv2/tflite\\_int8/vwv2\\_50\\_50\\_INT8.tflite](https://github.com/ARM-software/ML-zoo/blob/master/models/visual_wake_words/micronet_vwv2/tflite_int8/vwv2_50_50_INT8.tflite)

<sup>6</sup><https://github.com/ARM-software/ML-zoo>

<sup>7</sup>[https://hanlab.mit.edu/projects/tinyml/mcunet/release/mcunet-10fps\\_vwv.tflite](https://hanlab.mit.edu/projects/tinyml/mcunet/release/mcunet-10fps_vwv.tflite)

<sup>8</sup><https://github.com/mit-han-lab/mcunet>

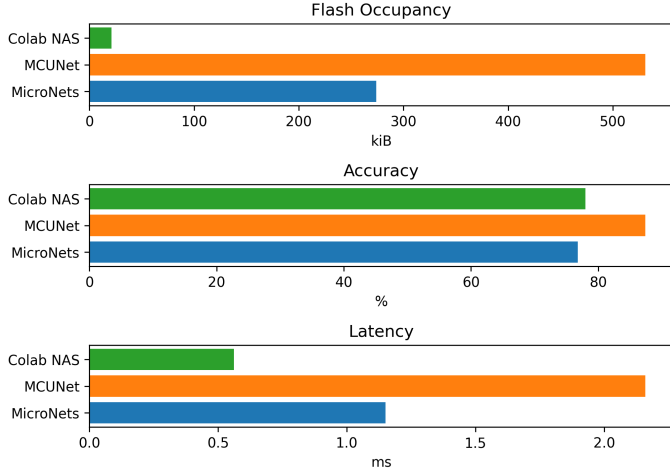


Figure 9: Graphical representation of the state-of-the-art comparison.

thanks to the Netron web application. Accuracy is evaluated on the minival image ids of COCO2014 dataset [15], which were not included in the training set, as done by Chowdhery et al. [13].

	Flash	Acc	input	latency
MicroNets	274kiB	76.8	50x50x1	1.15 ms
MCUNet	531kiB	87.4	64x64x3	2.16 ms
Our	21 kiB	78	50x50x3	561 $\mu$ s

Our network improves by all means the one proposed by MicroNets. However, the solution proposed by MCUNet is still more accurate. It offers 9.4 per cent points more accuracy than our solution while being 3.9 times slower and 25.3 times bigger.

### 7.1. Search Costs Comparison

As stated by Lin et al. [1] MCUNet spent 300 GPU hours to produce its architecture. Instead, MicroNets by Banbury et al. [2] does not declare the time spent on finding the architecture. However, they run DNAS for 200 epochs to find it. Differentiable NAS (DNAS) by Liu et al. [26], uses 1.5 GPU days (does not include the selection cost (1 GPU day) or the final evaluation cost by training the selected architecture from scratch (1.5 GPU days)) to find a network over the CIFAR-10 dataset, which contains 60000 32x32 colour images in 10 classes, with 6000 images per class. In this case, DNAS is run for 100 epochs. Considering that the visual wake word training set is composed of 107,954 images, that the input volume used is 50x50x1 and that the epochs used are double, the time spent on it is higher than the time spent on the CIFAR-10. Hence the NAS proposed in this article results much faster than MCUNet and MicroNets.

## 8. Conclusion

In this paper, we proposed Colab NAS: an affordable HW NAS technique for designing task-specific CNNs. Its novel search strategy, inspired by Occam’s razor, has a low search

cost. It obtains state-of-the-art results on the visual wake word dataset in just 4.5 GPU hours, improving, by all means, the solution found by MicroNets.

The low search cost allows its execution on free online services such as Kaggle Kernel or Google Colaboratory, without owning a high-end GPU. Given the current global chip shortage, this can help those end-users and researchers who want to approach application of lightweight CNNs for custom classification problems.

It also provides task-specific lightweight CNNs that are on average 156.2 times smaller and perform 10.5 times fewer FLOPs than those obtained by applying transfer learning based on MobileNetV2 on the same task, one of the most used techniques in 2022 to obtain task-specific lightweight CNNs in research. This is at the cost of losing 0.018 accuracy points on average. Such a trade-off can target deployment on the growing field of wearable and distributed devices with embedded electronics hardware. Moreover, reducing the computational cost of the final application turns into more efficient power consumption. In a world where artificial intelligence is becoming more and more diffused, reducing energy consumption is a fundamental step towards a more sustainable future.

## References

- [1] J. Lin, W. M. Chen, H. Cai, C. Gan, and S. Han, Memory-efficient Patch-based Inference for Tiny Deep Learning, *Advances in Neural Information Processing Systems*, 34, 2346-2358, 2021.
- [2] C. Banbury, C. Zhou, I. Fedorov, R. Matas, U. Thakker, D. Gope, V. j. Reddi, M. Mattina, and P. Whatmough, Micronets: Neural network architectures for deploying tinyml applications on commodity micro-controllers. *Proceedings of Machine Learning and Systems*, 3, 517-532, 2021.
- [3] T. Sanida, A. Sideris, D. Tsiktsiris and M. Dasygenis, Lightweight Neural Network for COVID-19 Detection from Chest X-ray Images Implemented on an Embedded System. *Technologies* 2022, 10, 37. <https://doi.org/10.3390/technologies10020037>.
- [4] M. Sandler, A. Howard, M. Zhu, A. Zhmoginov and L. -C. Chen, MobileNetV2: Inverted Residuals and Linear Bottlenecks, 2018 IEEE/CVF Conference on Computer Vision and Pattern Recognition, pp. 4510-4520, doi: 10.1109/CVPR.2018.00474.
- [5] S. Liu, W. Kong, X. Chen, M. Xu, M. Yasir, L. Zhao and J. Li, Multi-Scale Ship Detection Algorithm Based on a Lightweight Neural Network for Spaceborne SAR Images. *Remote Sens.* 2022, 14, 1149. <https://doi.org/10.3390/rs14051149>.
- [6] Y. Wang, C. Bai, X. Qian, W. Liu, C. Zhu and L. Ge, A DC Series Arc Fault Detection Method Based on a Lightweight Convolutional Neural Network Used in Photovoltaic System. *Energies* 2022, 15, 2877. <https://doi.org/10.3390/en15082877>.
- [7] M. Tan and Q. V. Le, EfficientNet: Rethinking Model Scaling for Convolutional Neural Networks, *Proceedings of the 36th International Conference on Machine Learning*, PMLR 97:6105-6114, 2019.
- [8] S. Khaki, N. Safaei, H. Pham and L. Wang, WheatNet: A lightweight convolutional neural network for high-throughput image-based wheat head detection and counting, *Neurocomputing* 489, 78-89, 2022. <https://doi.org/10.1016/j.neucom.2022.03.017>.
- [9] F. Jubair, O. Al-karadsheh, D. Malamos, S. Al Mahdi, Y. Saad and Y. Hassona, A novel lightweight deep convolutional neural network for early detection of oral cancer. *Oral Dis.* 2022; 28: 1123– 1130. <https://doi.org/10.1111/odi.13825>
- [10] E. Ragusa, T. Apicella, C. Gianoglio, R. Zunino and P. Gastaldo, Design and Deployment of an Image Polarity Detector with Visual Attention. *Cogn Comput* 14, 261–273 (2022). <https://doi.org/10.1007/s12559-021-09829-6>

- [11] E. Ragusa, C. Gianoglio, S. Dosen and P. Gastaldo, Hardware-Aware Affordance Detection for Application in Portable Embedded Systems, in *IEEE Access*, vol. 9, pp. 123178-123193, 2021, doi: 10.1109/ACCESS.2021.3109733.
- [12] J. Deng, W. Dong, R. Socher, L. -J. Li, Kai Li and Li Fei-Fei, ImageNet: A large-scale hierarchical image database, 2009 IEEE Conference on Computer Vision and Pattern Recognition, 2009, pp. 248-255, doi: 10.1109/CVPR.2009.5206848.
- [13] A. Chowdhery, P. Warden, J. Shlens, A. Howard and R. Rhodes, Visual wake words dataset, 2019, arXiv preprint, arXiv:1906.05721.
- [14] C. R. Banbury, V. J. Reddi, M. Lam, W. Fu, A. Fazel, J. Holleman, ... and P. Yadav, Benchmarking TinyML systems: Challenges and direction, 2020, arXiv preprint arXiv:2003.04821.
- [15] T.Y. Lin, et al. Microsoft coco: Common objects in context. European conference on computer vision. Springer, Cham, 2014.
- [16] C. Banbury, F. Zhou, I. Fedorov, R. Matas, U. Thakker, D. Gope, V. Janapa Reddi, M. Mattina and P. Whatmough, MicroNets: Neural Network Architectures for Deploying TinyML Applications on Commodity Microcontrollers, *Proceedings of Machine Learning and Systems*, p.p. 517-532, v. 3, 2021
- [17] M. Lin, Q. Chen and S. Yan, Network In Network, 2014, CoRR, abs/1312.4400.
- [18] M. Shanker, M.Y. Hu and M.S. Hung, Effect of data standardization on neural network training, *Omega*, Volume 24, Issue 4, 1996, Pages 385-397, [https://doi.org/10.1016/0305-0483\(96\)00010-2](https://doi.org/10.1016/0305-0483(96)00010-2).
- [19] S. Ioffe and C. Szegedy, Batch normalization: Accelerating deep network training by reducing internal covariate shift, 1996, PMLR, 37:448-456.
- [20] D.P. Kingma, and J. Ba, Adam: A Method for Stochastic Optimization, 2015, CoRR, abs/1412.6980.
- [21] X. Xu, Y. Ding, S.X. Hu, et al. Scaling for edge inference of deep neural networks. *Nat Electron* 1, 216–222 2018. <https://doi.org/10.1038/s41928-018-0059-3>.
- [22] S. S. Saha, S. S. Sandha and M. Srivastava, Machine Learning for Microcontroller-Class Hardware: A Review, 2022, arXiv preprint arXiv:2205.14550.
- [23] N. S. Keskar, D. Mudigere, J. Nocedal, M. Smelyanskiy, and P. T. P. Tang, On large-batch training for deep learning: Generalization gap and sharp minima, 2016, arXiv preprint arXiv:1609.04836.
- [24] J. Lin, W. M. Chen, Y. Lin, J. Cohn, C. Gan, and S. Han, Mncunet: Tiny deep learning on iot devices, in *Advances in Neural Information Processing Systems (NeurIPS'20)*, 2020.
- [25] M. Tan, B. Chen, R. Pang, V. Vasudevan, and Q. V. Le, Mnasnet: Platform-aware neural architecture search for mobile, CoRR, vol. abs/1807.11626, 2018.
- [26] H. Liu, K. Simonyan, and Y. Yang, "DARTS: differentiable architecture search," in 7th International Conference on Learning Representations, ICLR, 2019.
- [27] H. Cai, L. Zhu, and S. Han, Proxylessnas: Direct neural architecture search on target task and hardware, CoRR, vol. abs/1812.00332, 2018.
- [28] A. G. Howard, M. Zhu, B. Chen, D. Kalenichenko, W. Wang, T. Weyand, M. Andreetto, and H. Adam. Mobilenets: Efficient convolutional neural networks for mobile vision applications. arXiv preprint arXiv:1704.04861, 2017.
- [29] M. Sandler, A. Howard, M. Zhu, A. Zhmoginov, and L.C. Chen. Mobilenetv2: Inverted residuals and linear bottlenecks. CVPR, 2018.
- [30] A. Howard, M. Sandler, G. Chu, L. C. Chen, B. Chen, M. Tan, W. Wang, Y. Zhu, R. Pang, V. Vasudevan, Q. V. Le and H. Adam, Searching for mobilenetv3, In *Proceedings of the IEEE/CVF international conference on computer vision*, pp. 1314-1324, 2019
- [31] F. N. Iandola, S. Han, M. W. Moskewicz, K. Ashraf, W. J. Dally, and K. Keutzer. Squeezenet: Alexnet-level accuracy with 50x fewer parameters and 0.5 mb model size. arXiv preprint arXiv:1602.07360, 2016.
- [32] X. Zhang, X. Zhou, M. Lin, and J. Sun. Shufflenet: An extremely efficient convolutional neural network for mobile devices. CVPR, 2018.
- [33] N. Ma, X. Zhang, H. T. Zheng, and J. Sun. Shufflenet v2: Practical guidelines for efficient cnn architecture design. ECCV, 2018.